Fusion Engineering and Design 125 (2017) 396–401

Contents lists available at ScienceDirect

Fusion Engineering and Design

journal homepage: www.elsevier.com/locate/fusengdes

Helium bubble formation behavior in ODS ferritic steels with and without simultaneous addition of Al and Zr

Peng Song[a,*], Zhexian Zhang[b], Kiyohiro Yabuuchi[b], Akihiko Kimura[b]

[a] Graduate School of Energy Science, Kyoto University, Yoshida-honmachi, Sakyou-ku, Kyoto 606-8501, Japan
[b] Institute of Advanced Energy, Kyoto University, Gokasho, Uji, Kyoto 611-0011, Japan

HIGHLIGHTS

- He effects were studied for two ODS ferritic steels with/without simultaneous addition of Al and Zr.
- Trapping effects of oxide particles, grain boundaries, dislocations on He atoms were discussed.
- Oxide particles with a high sink strength contribute to enhanced swelling resistance.

ARTICLE INFO

Article history:
Received 30 October 2016
Received in revised form 21 March 2017
Accepted 23 March 2017
Available online 3 April 2017

Keywords:
ODS steel
He irradiation
Swelling
Sink strength

ABSTRACT

Two 14.5 wt.% Cr-ODS ferritic steels with and without simultaneous addition of 3.5 wt.% Al and 0.27 wt.% Zr were irradiated with He^+ up to 0.2 dpa/3500 appm at 300 °C, 550 °C, 700 °C in order to investigate the effects of Al and Zr addition on He bubble formation behavior in 14.5Cr-ODS ferritic steel. The mean grain size of each ODS steel was about 370 nm. Al addition resulted in the formation of larger oxide particles with a lower number density in 14.5Cr-ODS ferritic steel. After irradiation to 0.2 dpa/3500 appm He, dislocation densities in both ODS ferritic steels showed no change. However, the size and number density of He bubbles were increased and decreased, respectively, by the simultaneous addition of Al and Zr. Although both ODS steels showed good resistance to He-bubble induced swelling, the 14.5Cr-ODS steel possessed a better swelling resistance than 14.5Cr-3.5 Al (Zr)-ODS steel. It was considered that the oxide particles were the main contributor for the swelling resistance of ODS steels by providing a number of defect sinks with a high sink strength. The swelling increased with increasing irradiation temperature in both ODS steels, indicating that the de-trapping He enhanced He-bubble swelling.

1. Introduction

Oxide dispersion strengthened (ODS) steels with a high number density of nano-scaled oxide particles as well as fine grains show excellent mechanical properties, remarkable thermal stability and attractive radiation tolerance [1–5]. Moreover, in comparison to the leading candidate blanket structural material, reduced activation ferritic/martensitic (RAFM) steels, ODS steels possess outstanding creep strength at elevated temperatures up to about 700 °C, and overcome radiation tolerance after neutron irradiation up to 50 dpa [1,5]. Therefore, ODS steels are another possible candidate structural materials to expand the design margin of the blanket and to improve thermal efficiency of future fusion reactors. Concerning the materials issues of blanket structural materials, the effects of transmuted helium, such as bubble formation and grain boundary He precipitation, are unavoidable. Therefore, a profound understanding of helium effects is essential for improving the performance of the candidate blanket structural materials.

As for swelling in ODS steels, several ODS steels were studied under single heavy ion irradiation, single He ion irradiation and multi-beam ion irradiation [6–11]. M.B. Toloczko [6] has demonstrated the excellent swelling resistance of ODS ferritic alloy MA957 by showing its low void swelling of only 4.5% even after irradiation to 500 dpa at 450 °C. Under Fe/He dual-ion irradiation, ODS alloys were more resistant to void swelling than non-ODS RAFM steels because of a lower dislocation bias and a high number density of fine oxide particles acting as effective traps for He atoms and vacancies [7,8]. Moreover, much lower void swelling was found in tempered martensite grains than ferrite grains for 12Cr ODS ferritic-martensitic alloy after 800 dpa iron-ion irradiation, which should stem from the high density internal boundaries of tempered

* Corresponding author.
E-mail addresses: p-song@iae.kyoto-u.ac.jp, songpeng1123@gmail.com (P. Song).

http://dx.doi.org/10.1016/j.fusengdes.2017.03.139
0920-3796/

Table 1
Chemical compositions of 14.5Cr-3.5Al (Zr)-ODS and 14.5Cr-ODS ferritic steels.

Elements	Fe	Cr	W	Ti	Al	Zr	Y_2O_3
14.5Cr-3.5Al (Zr)-ODS	Bal.	14.59	1.84	0.14	3.46	0.27	0.33
14.5Cr-ODS	Bal.	13.6	1.9	0.16	–	–	0.33

Symbol "-" means the absence of an alloying element in the ODS steel.

martensite [9]. Accordingly, it was summarized that microstructures such as; oxide particles, dislocations and grain boundaries, played a vital role in suppressing void swelling in ODS steels. Unlike heavy ion irradiation, He ion implantation generally produces a smaller number of atomic displacements thus causing fewer damage structures. With regard to swelling behavior of ODS steels under helium irradiation, W. Xu et al. elucidated a relationship between oxide particle and He bubble induced swelling of ODS alloys, that the swelling went up with oxide particle diameter [10]. Before that, T. Yamamoto et al. have obtained strong evidence for the existence of a high number density of ultrafine He bubbles trapped on nano-sized YTiO particles at 500 °C [11]. However, few researchers have reported temperature dependent swelling in ODS steels irradiated with a large amount of He.

Concerning Al-containing ODS steels, they might not be adequate for the application to fusion blanket which demands reduced activation [12]. However, the simultaneous addition of Al and Zr to 16Cr-ODS steels improved not only corrosion resistance but also high-temperature strength up to the almost same level with 16Cr-ODS steels [1]. Moreover, 16Cr-4Al-ODS steel with Zr addition was more resistant to the formation and growth of radiation-induced dislocation loops than 16Cr-4Al-ODS steel [13]. So Al and Zr alloyed high-Cr ODS ferritic steels could be feasible for applications to next generation nuclear systems. Actually, the changes in strength were due to the alteration of the sorts of the oxide particles, which resulted in a dispersion morphology change of the oxide particles. It is also expected that the swelling behavior is influenced by the sort of dispersed oxide particles.

The objective of this work is to investigate the effects of Al and Zr addition, which alters the oxide particle dispersion morphology, on the He-bubble induced swelling behavior of 14.5Cr ODS ferritic steel in order to understand the role of nano-scaled oxide particles in swelling resistance in ODS ferritic steels.

2. Materials and experimental methods

The materials used in this work were two 14.5Cr ODS ferritic steels, designated 14.5Cr-ODS and 14.5Cr-3.5Al (Zr)-ODS. The chemical compositions of the ODS ferritic steels are shown in Table 1. The 14.5Cr-3.5Al (Zr)-ODS steel contained 3.5 wt.% Al and 0.27 wt.% Zr as alloying elements. The main fabrication process is described in Ref. [14]. The final heat treatment was an annealing at 1150 °C for 1 h and air-cooled. The specimen surface for He-irradiation was ground with SiC papers down to 2000 grit, followed by polishing with successive grades of diamond spray down to 0.25 μm. Electro-polishing was finally conducted by using a solution composed of 5% (vol.) $HClO_4$ and 95% (vol.) CH_3COOH at room temperature for 30 s to remove the damaged layer produced by mechanical polishing.

He-irradiation experiments were carried out at the DuET facility at Kyoto University by using 1 MeV He^+ ions, whose energy was separated into 201 keV, 467 keV, 737 keV and 1 MeV by a rotating energy degrader made of thin Al foils, then injected into the samples to form a homogenous He atoms distribution. The fluence was roughly 4.5×10^{20} ions m^{-2} and the corresponding flux was about 6.2×10^{16} ions m^{-2} s^{-1}. The irradiation temperatures were 300 °C, 550 °C and 700 °C with a temperature fluctuation of ±10 °C, which was measured by a thermo-couple and an infrared thermography. At each temperature, the two ODS specimens were irradiated simultaneously for about 2 h.

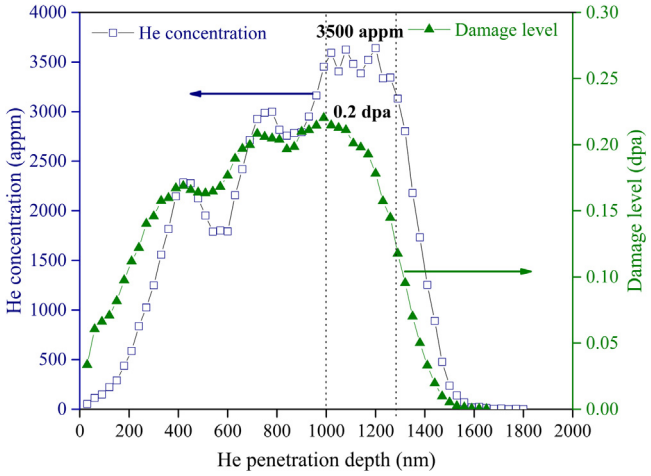

Fig. 1. Depth profiles of damage level (in units of displacements per atom, dpa) and He atom concentration (appm) calculated with SRIM code.

The He concentration and damage level as a function of the He-ions penetration depth were obtained by SRIM simulation [15], as shown in Fig. 1. For the depth ranging from 1000 to 1300 nm, the He concentration remained stable around 3500 appm. The corresponding nominal damage level was about 0.2 dpa.

The cross sectional specimens for transmission electron microscopy (TEM) observations were fabricated by the lift-out technique using a Focused Ion Beam (FIB), then treated by flash polishing or low energy Ar ion sputtering to eliminate FIB damage. TEM observation was done using a conventional 200 kV JEOL JEM 2010 microscope. The thickness of all TEM samples was acquired based on the measurement of fringe spacing in Convergent Beam Electron Diffraction (CBED) patterns.

The grain morphology was observed by the electron backscatter diffraction (EBSD) technique using ZEISS Ultra55 field emission scanning electron microscopy (FESEM) and the mean grain size was obtained from 3000 grains for each ODS steel.

3. Results and discussion

3.1. Grain morphology

The grain morphologies of the irradiation surfaces obtained by EBSD technique are shown in Fig. 2a and 2b for 14.5Cr-3.5Al (Zr)-ODS and 14.5Cr-ODS steels, respectively. Different colors represent different grains. In both steels, the grain sizes were not homogenous and most were less than 1 μm. The mean grain size of each ODS steel was estimated to be about 0.37 μm. Although the irradiation temperature was elevated to 700 °C in this work, no grain coarsening occurred because the grain boundaries were pinned down by fine oxide particles, which agrees with the previous work by Y. Ha [16] who reported that no recrystallization or evolution of oxide particles occurred in Al-added and Al-free ODS steels after annealing up to 1350 °C.

3.2. Oxide particles and dislocations

Dispersion morphologies of oxide particles in both ODS steels were observed by TEM using $\mathbf{g}=(110)$ at a two-beam condition with the deviation vector $\mathbf{s}_g \neq 0$, and shown in Fig. 3. The corresponding size distributions are presented in Fig. 3c. For 14.5Cr-3.5Al (Zr)-ODS, the mean diameter of oxide particles was 6.2 nm and the number density was 3.5×10^{22} m^{-3}. For 14.5Cr-ODS, smaller

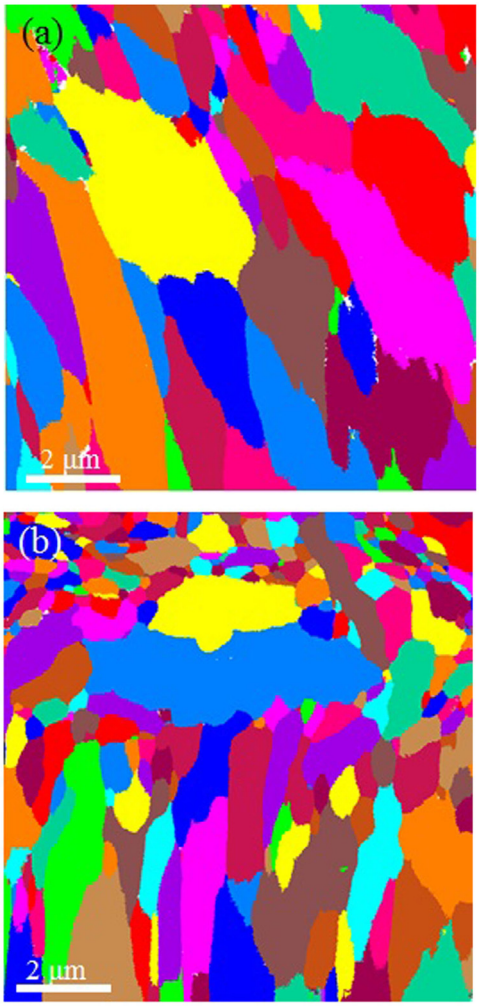

Fig. 2. Grain morphologies of (a) 14.5Cr-3.5Al (Zr)-ODS and (b) 14.5Cr-ODS.

Table 2
Dislocation densities (m^{-2}) of unirradiated samples and He-ions irradiated samples at 300 °C, 550 °C with a damage level of 0.2 dpa.

	Un-irradiated	300 °C	550 °C
14.5Cr-3.5Al (Zr)-ODS	1.4×10^{14}	1.3×10^{14}	0.8×10^{14}
14.5Cr-ODS	1.2×10^{14}	0.7×10^{14}	1.2×10^{14}

oxide particles of 3.0 nm were observed with a higher number density of 1.1×10^{23} m^{-3}. In Zr-free 15Cr-ODS steels, the Al addition resulted in the alteration of oxide particles from nanoscale pyrochlore ($Y_2Ti_2O_7$) oxides to larger yttrium aluminum perovskite (YAP, $YAlO_3$) and yttrium aluminum hexagonal (YAH, $YAlO_3$) oxides [17]. The simultaneous addition of Al and Zr, however, suppressed the nucleation of Y-Al oxides and enhanced the formation of Y-Zr oxides [1]. As for the effect of irradiation on the oxide particles in this work, the dispersion morphologies were not changed by irradiation, which is also consistent with the previous work indicating that they remained stable even after irradiation up to 150 dpa at 670 °C [18].

The dislocations before irradiation were observed by TEM using vector **g** = (110) under pole [001] and could be seen in Fig. 3a and b. After He ion irradiation at 300 and 550 °C, dislocations were observed at a depth range of 1000–1300 nm. The measured dislocation densities before and after irradiation are summarized in Table 2, indicating no significant change among them for a damage level of about 0.2 dpa. Above 300 °C (greater than 0.2 T_M, where T_M is the melting temperature), vacancies detrapped from impurities and might accelerate mutual annihilation with interstitial atoms. As a result, few defects survived to form dislocation structures after collision cascades [19].

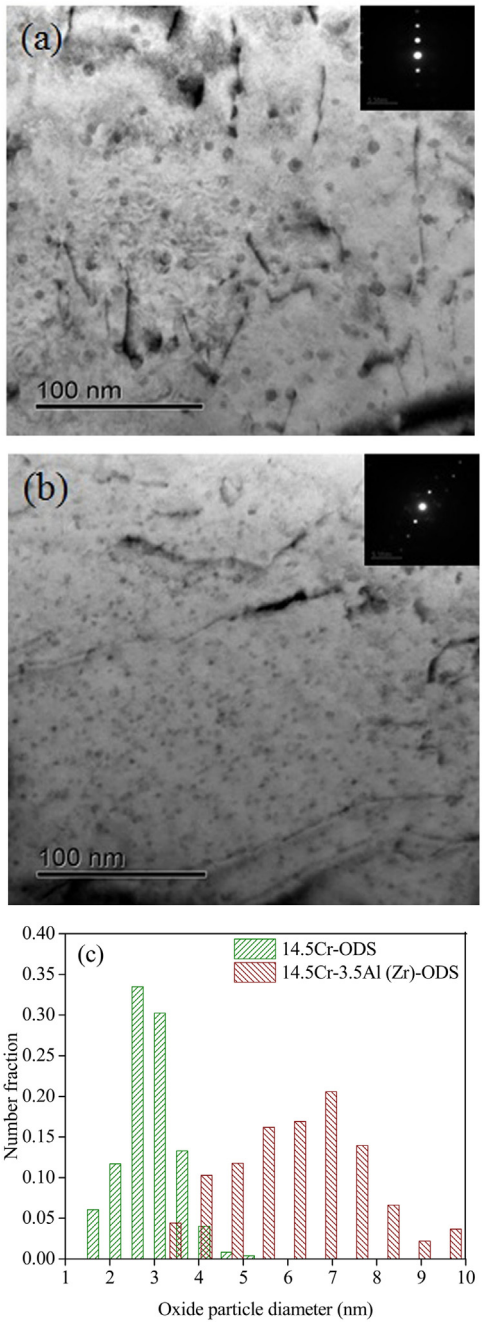

Fig. 3. Bright-field images of dislocations and oxide particles in (a) 14.5Cr-3.5Al (Zr)-ODS, (b) 14.5Cr-ODS taken under a two-beam diffraction condition by using **g** = 110 and (c) size distribution histogram of oxide particles.

3.3. He bubbles

He bubbles in the depth range from 1000 to 1300 nm were observed under defocused conditions (see Fig. 4). The irradiation temperature dependences of mean diameter and number density of He bubbles are displayed in Fig. 5a and b, respectively. In both steels, the bubble size and number density increased and decreased, respectively, with increasing irradiation temperature. At 300 °C,

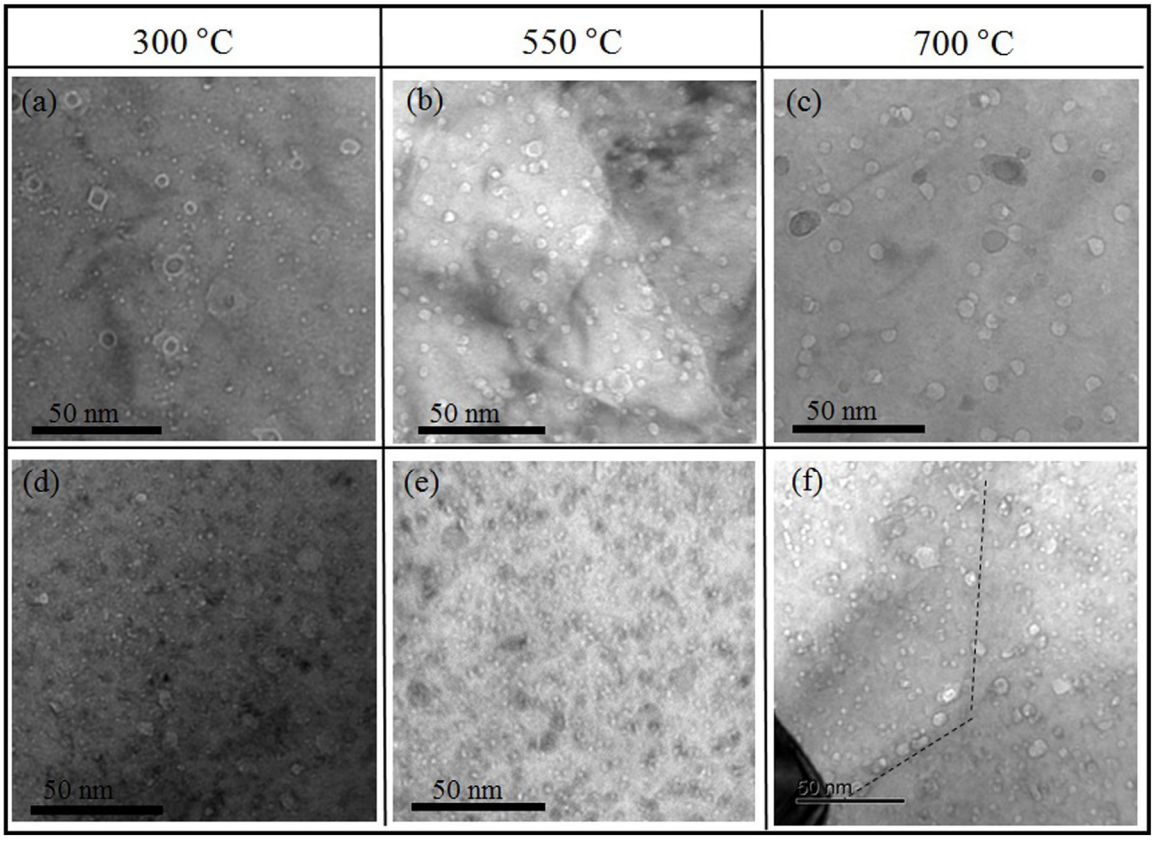

Fig. 4. TEM micrograph of He bubbles in 14.5Cr-3.5Al (Zr)-ODS (a) to (c) and 14.5Cr-ODS (d) to (f) taken at under-focus conditions, the He concentration of around 3500 appm.

some tiny spherical bubbles were nucleated along dislocation lines as shown in Fig. 4a, implying that He atoms were trapped at dislocations. In Fig. 4d, only the isolate spherical He bubbles existed. For both the ODS ferritic steels, the average diameter of He bubbles was about 1.6 nm. Actually, at 300 °C, He-vacancy clusters smaller than He_3V_5 were mobile but their diffusion coefficients were at least two orders of magnitude lower than that of a mono vacancy [20].

At 550 °C (over 0.3 T_M), He bubbles grew up evidently and were of mean diameter 5.0 nm with some loss of spherical shape in 14.5Cr-3.5Al (Zr)-ODS (in Fig. 4b). No obvious size difference was found between intragranular and intergranular bubbles. In 14.5Cr-ODS, bubbles grew very slightly (see Fig. 4e and Fig. 5a) with increasing temperature.

At 700 °C, He bubble size became the largest. In Fig. 4f, intergranular bubbles (near the black dash) were bigger than intragranular bubbles in 14.5Cr-ODS steel, indicating that the bubble growth on grain boundary was more favorable than in the grain. Under high temperature conditions (more than 0.5 T_M), He-vacancy complexes smaller than the critical size were not thermally stable. Furthermore, more vacancies flew to stable He bubbles having a size bigger than the critical value. As a result, He bubbles grew with a low number density.

3.4. Swelling behavior

In the depth range of 1000–1300 nm, the local swelling ($\Delta V/V$) induced by He bubbles can be approximately defined as follows:

$$\Delta V/V = (4/3)\pi R^3 \rho \quad (1)$$

where R and ρ are the average radius and the number density of He bubbles, respectively [21]. All swelling values of ODS ferritic steels are shown in Fig. 5c as a function of irradiation temperature.

At 300 °C, both ODS steels exhibited a near-zero swelling. As the temperature increased, the swelling of 14.5Cr-ODS steel tended to be saturated but that of 14.5Cr-3.5Al (Zr)-ODS steel continued to increase. The largest swelling of the latter steel was less than 0.7% at 700 °C, which is in accordance with the largest value of 0.5% in 15CRA3 ODS alloy irradiated to about 3300 appm He at 500 °C [22]. At each irradiation temperature, the swelling was smaller in 14.5Cr-ODS steel than 14.5Cr-3.5Al (Zr)-ODS steel.

Microstructures, including dislocations, dislocation loops, grain boundaries, and oxide particles may contribute to swelling resistance by playing a role as sinks for radiation induced damage structures. The sink strength of dislocation lines for point defects is approximately estimated as the dislocation density (about 1.4×10^{14} m^{-2}), whilst that of oxide particles Z_s is expressed by $4\pi r_s N_s$ [2,3], where r_s is the mean radius and N_s is the number density. Accordingly, the sink strengths of oxide particles in 14.5Cr-3.5Al (Zr)-ODS and 14.5Cr-ODS steels were 1.4×10^{15} m^{-2} and 2.1×10^{15} m^{-2}, respectively. In general, dislocations can preferentially absorb interstitials (He or Fe atoms) over vacancies. This effect could become more efficient especially at lower temperatures. However, in this work, when compared to the capture efficiency of oxide particles, the dislocation bias effect was rather negligible. In terms of the influence of grain boundaries on swelling resistance, M.B. Toloczko et al. discovered distinguishable void-denuded zones near grain boundaries, which led to a reduction of the overall swelling of MA957 ODS at 500 dpa [6]. But void-denuded zones were not observed in the current work. Taking into account the similar grain morphologies of both steels and larger intergranular bubbles in 14.5Cr-ODS ferritic steels, oxide particles should play a crucial role in causing discrepancies in swelling resistance for these two ferritic ODS steels.

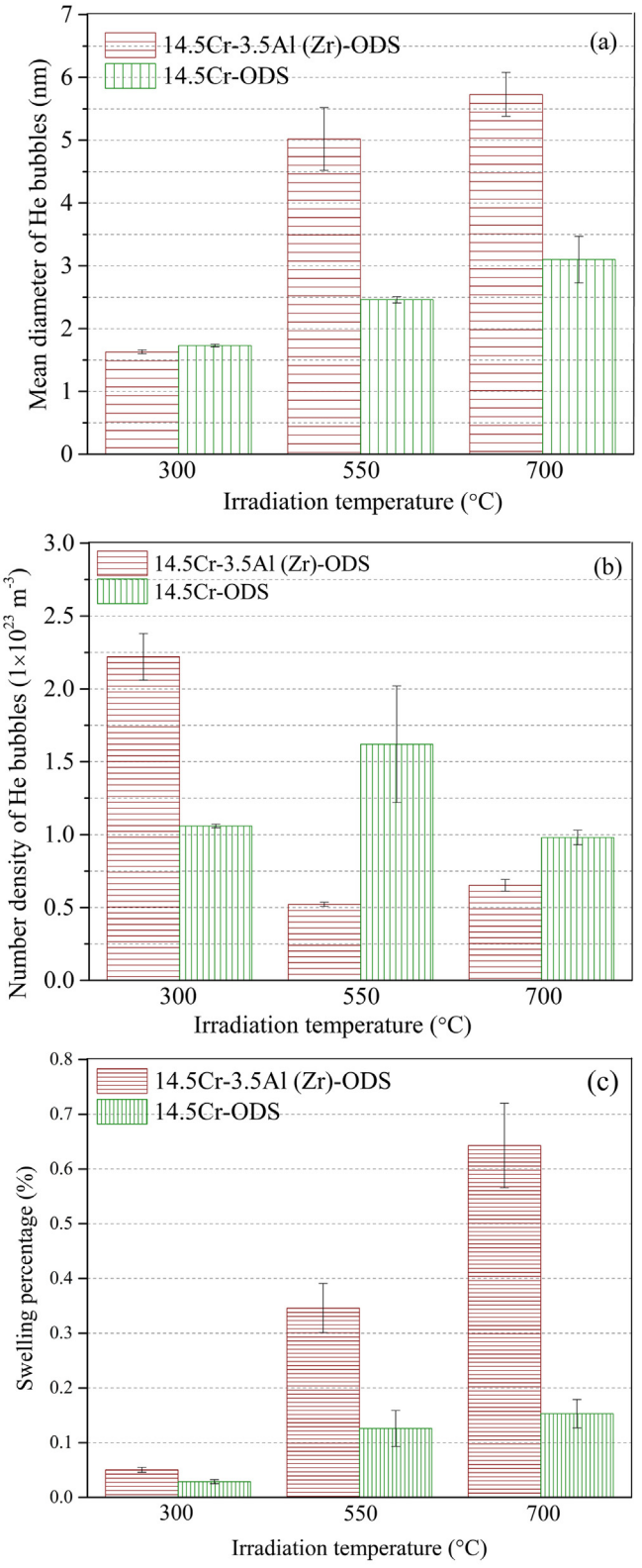

Fig. 5. The mean bubble size, number density and void swelling as a function of irradiation temperature for two ODS ferritic steels.

In addition, it was elucidated by kinetic rate theory that void swelling was characterized by a peak at an intermediate irradiation temperature. Meanwhile, temperature sensitive parameters, the vacancy diffusion coefficient and the equilibrium vacancy concentration, controlled the process of void growth [21]. This phenomenon was also observed in He or Fe ions irradiated ODS steels and non-ODS steels [6,22,23]. In other words, similar to void swelling, it is possible for He bubble swelling to have an analogical dependence on temperature. At low temperatures, the limited mobility of vacancies, their clusters and He-vacancy complexes restrained the growth of bubbles, then suppressing swelling. With increasing temperature, vacancies became mobile and the swelling might reach its maximum value. For ODS steels, oxide particles trapped He atoms and vacancies keeping the size of He bubbles small by acting as sinks for He and vacancies. In our work, the saturation temperature of swelling tended to be higher for 14.5Cr-3.5Al (Zr)-ODS ferritic steel than for 14.5Cr-ODS ferritic steel. This might be related to the higher capture efficiency of oxide particles in 14.5Cr-ODS ferritic steel. Therefore, controlling the dispersion morphology of oxide particles with a high sink strength is necessary to enhance swelling resistance.

4. Conclusions

He bubble formation behaviors were compared between two ODS ferritic steels with and without simultaneous addition of Al and Zr after irradiation with 3500 appm He ions up to 0.2 dpa at 300 °C, 550 °C, 700 °C. The obtained main results are as follows:

1) In both steels, the grain sizes were not homogenous and most were less than 1 μm. The mean grain size of each ODS steel was estimated to be about 0.37 μm. For 14.5Cr-3.5Al (Zr)-ODS, the mean diameter of oxide particles was 6.2 nm and the number density was 3.5×10^{22} m^{-3}, while in 14.5Cr-ODS, smaller oxide particles of 3.0 nm existed with a higher number density of 1.1×10^{23} m^{-3}.
2) Dislocation densities were mostly similar both before and after irradiation.
3) In both steels, the bubble sizes and number densities increased and decreased, respectively, with increasing irradiation temperature. At 300 °C, some tiny spherical bubbles were nucleated along dislocation lines, implying that He atoms were trapped at dislocations. At 550 °C, He bubbles grew to 5.0 nm in diameter. At 700 °C, He bubble size became the largest.
4) At 300 °C, two ODS steels exhibited a near-zero swelling. As the temperature increased, the swelling of 14.5Cr-ODS steel tended to be saturated but that of 14.5Cr-3.5Al (Zr)-ODS steel continued to increase. The largest swelling of the latter steel was less than 0.7% at 700 °C. At each irradiation temperature, the swelling was smaller in 14.5Cr-ODS steel than in 14.5Cr-3.5Al (Zr)-ODS steel.
5) Taking into account the similar grain morphologies of both the steels and larger intergranular bubbles in 14.5Cr-ODS ferritic steels, oxide particles played a crucial role in causing discrepancies in swelling resistance for these two ferritic ODS steels. Therefore, controlling the dispersion morphology of oxide particles with a high sink strength is necessary to enhance swelling resistance.

Acknowledgments

The first author wishes to acknowledge Japanese Government (MEXT) for scholarship and the China Scholarship Council for their kind support. The authors are also grateful to the technical support by members of Application of Duet and Muster for Industrial Research and Engineering (ADMIRE), Kyoto University.

References

[1] A. Kimura, R. Kasada, N. Iwata, et al., Development of Al added high-Cr ODS steels for fuel cladding of next generation nuclear systems, J. Nucl. Matter. 417 (2011) 176–179.

[2] G.R. Odette, D.T. Hoelzer, Irradiation-tolerant nanostructured ferritic alloys: transforming helium from a liability to an asset, JOM 62 (2010) 84–92.
[3] G.R. Odette, M.J. Alinger, B.D. Wirth, Recent developments in irradiation-resistant steels, Annu. Rev. Mater. Res. 38 (2008) 471–503.
[4] S. Ukai, M. Fujiwara, Perspective of ODS alloys application in nuclear environments, J. Nucl. Mater. 307–311 (2002) 749–757.
[5] S.J. Zinkle, J.T. Busby, Structural materials for fission & fusion energy, Mater. Today 12 (2009) 12–19.
[6] M.B. Toloczko, F.A. Garner, V.N. Voyevodin, et al., Ion-induced swelling of ODS ferritic alloy MA957 tubing to 500 dpa, J. Nucl. Mater. 453 (2014) 323–333.
[7] I.-S. Kim, J.D. Hunn, N. Hashimoto, et al., Defect and void evolution in oxide dispersion strengthened ferritic steels under 3.2 MeV Fe^{+} ion irradiation with simultaneous helium injection, J. Nucl. Mater. 280 (2000) 264–274.
[8] K. Yutani, H. Kishimoto, R. Kasada, et al., Evaluation of Helium effects on swelling behavior of oxide dispersion strengthened ferritic steels under ion irradiation, J. Nucl. Mater. 367–370 (2007) 423–427.
[9] T. Chen, E. Aydogan, J.G. Gigax, et al., Microstructural changes and void swelling of a 12Cr ODS ferritic-martensitic alloy after high-dpa self-ion irradiation, J. Nucl. Mater. 467 (2015) 42–49.
[10] W. Xu, L. Li, J.A. Valdez, et al., Effect of nano-oxide particle size on radiation resistance of iron-chromium alloys, J. Nucl. Mater. 469 (2016) 72–81.
[11] T. Yamamoto, G.R. Odette, P. Miao, et al., The transport and fate of helium in nanostructured ferritic alloys at fusion relevant He/dpa ratios and dpa rates, J. Nucl. Mater. 367–370 (2007) 399–410.
[12] R.H. Jones, H.L. Heinisch, K.A. McCarthy, Low activation materials, J. Nucl. Mater. 271–272 (1999) 518–525.
[13] C.Z. Yu, H. Oka, N. Hashimoto, et al., Development of damage structure in 16Cr-4Al ODS steels during electron-irradiation, J. Nucl. Mater. 417 (2011) 286–288.
[14] P. Dou, A. Kimura, R. Kasada, et al., TEM and HRTEM study of oxide particles in an Al-alloyed high-Cr oxide dispersion strengthened steel with Zr addition, J. Nucl. Mater. 444 (2014) 441–453.
[15] http://www.srim.org/.
[16] Y. Ha, Recrystallization Behavior of Oxide Dispersion Strengthened Ferritic Steels. Doctoral Thesis, Kyoto University, 2014, pp. 72–96.
[17] P. Dou, A. Kimura, T. Okuda, et al., Polymorphic and coherency transition of Y–Al complex oxide particles with extrusion temperature in an Al-alloyed high-Cr oxide dispersion strengthened ferritic steel, Acta Mater. 59 (2011) 992–1002.
[18] H. Kishimoto, K. Yutani, R. Kasada, et al., Heavy-ion irradiation effects on the morphology of complex oxide particles in oxide dispersion strengthened ferritic steels, J. Nucl. Mater. 367–370 (2007) 179–184.
[19] S.J. Zinkle, L.L. Snead, Designing radiation resistance in materials for fusion energy, Annu. Rev. Mater. Res. 44 (2014) 241–267.
[20] V.A. Borodin, P.V. Vladimirov, Diffusion coefficients and thermal stability of small helium–vacancy clusters in iron, J. Nucl. Mater. 362 (2007) 161–166.
[21] G.S. Was, Fundamentals of Materials Science Metals and Alloys, Springer, Berlin Heidelberg New York, 2007.
[22] L. Fave, M.A. Pouchon, M. Döbeli, et al., Helium ion irradiation induced swelling and hardening in commercial and experimental ODS steels, J. Nucl. Mater. 445 (2014) 235–240.
[23] E. Getto, Z. Jiao, A.M. Monterrosa, et al., Effect of pre-implanted helium on void swelling evolution in self-ion irradiated HT9, J. Nucl. Mater. 462 (2015) 458–469.